Sensors **2012**, *12*, 10369-10380; doi:10.3390/s120810369

OPEN ACCESS

sensors

ISSN 1424-8220

www.mdpi.com/journal/sensors

Article

A Multi-Parameter Decoupling Method with a Lamb Wave Sensor for Improving the Selectivity of Label-Free Liquid Detection †

Lianqun Zhou [1,2,3], Yihui Wu [1,2,*], Ming Xuan [1,2], Jean-François Manceau [3] and François Bastien [3]

1 Suzhou Institute of Biomedical Engineering and Technology, Chinese Academy of Sciences, Suzhou 215163, China; E-Mails: zhoulq@sibet.ac.cn (L.Z.); xuanm@ciomp.ac.cn (M.X.)

2 State Key Laboratory of Applied Optics, Changchun Institute of Optics, Fine Mechanics and Physics, Chinese Academy of Sciences, Changchun 130033, China

3 Institute FEMTO-ST, CNRS, Université de Franche-Comté, Besançon 25044, France; E-Mails: jfmanceau@femto-st.fr (J.-F.M.); fbastien@femto-st.fr (F.B.)

† Earlier version of this paper appears in the *16th International Conference on Solid-State Sensors, Actuators and Microsystems*, Beijing, China, 5–9 June 2011.

* Author to whom correspondence should be addressed; E-Mail: yihuiwu@ciomp.ac.cn; Tel.: +86-512-6958-8061; Fax: +86-512-6958-8058.

Received: 17 June 2012; in revised form: 17 July 2012 / Accepted: 24 July 2012 / Published: 31 July 2012

Abstract: In this paper, a liquid multi-parameter decoupling method with only one Lamb wave sensor is presented. In a Lamb wave sensor, antisymmetric modes (A_{01} mode for low frequency, A_{03} mode for high frequency) and symmetric modes (S_0 mode) are used to detect multiple parameters of a liquid, such as its density, sound velocity, and viscosity. We found they can play very different roles in the detections. For example, the A_{01} mode is very sensitive to the liquid's density but the A_{03} mode is sensitive to the sound velocity. Here, the A_0 mode is used to identify the density of the detected liquid and with this density value we obtained the viscosity by the amplitude shifts of the S_0 mode. This could be a way to distinguish an unknown liquid with high sensitivity or to solve the problem of selectivity of label-free detection on biosensors.

Keywords: Lamb wave sensor; density; sound velocity; viscosity; determination of multi-parameters

1. Introduction

Acoustic sensors have been widely used in chemical/biological fields with the label-free detection method to detect the mass changes on the sensor surface [1–17]. However, the selectivity of this method is often poor due to the absorption of non-target molecules, which are difficult to distinguish using only one-parameter sensors [18,19]. This has been a common problem of all kinds of label-free biosensors. The detection of multiple parameters using a multi-mode acoustic sensor significantly improves the label-free detection method. Acoustic waves which travel in a medium can have multiple modes and this character has been successfully used in a combined detection of density and viscosity for high viscosity solutions [20]. However, for low viscosity solutions like aqueous electrolytic solutions or bio liquids, it is still a challenge [9,20–24].

The micro Lamb wave sensor is a powerful tool for liquid detection because it is easier to get multi-mode vibration, and it performs with high sensitivity and low attenuation [25–29]. The two well-known basic modes, the antisymmetric mode (A_0 mode) and the symmetric mode (S_0 mode), have already been used for solving the problem of temperature compensation on a chip by the authors of [26,30]. The A_0 mode has been used to measure the concentration of bio/chemical liquids, such as the concentration of methanol for direct methanol cell applications [18]. However, it shows uncertain frequency shifts direction with the concentration changes of the liquid [18,31]. In fact, the parameters of a liquid, like the density, acoustic sound velocity and viscosity, will work together for a mode. So it's hard to decouple them with only one mode.

In this work, both the antisymmetric mode and the symmetric modes are used to decouple the liquid physical parameters. The characters of A_{03} mode, with a wavelength of about one-third of A_{01} mode (low frequency of A_0 mode), are investigated with the liquid loading for the first time. In order to discuss the response of Lamb wave sensor to the liquid loading, two types of experiments were set up. The first experiment was used to measure the frequency shifts with the same type of solutions with different concentrations loaded on the sensors' surface, such as the solutions of NaCl. It shows that the characters of the modes are very different. Although both A_{01} and A_{03} modes belong to A_0 mode, their frequency shifts showed an opposite behavior with the increase of the concentration of the loading solutions. The second experiment was used to measure the frequency changes with different types of solutions and different concentrations, such as solutions of KCl, NaBr and KBr. Although the tested objects are two different kinds of solutions with different concentrations, the frequency of A_{01} mode shows almost has no movement and A_{03} mode frequency shows a great difference. The frequency shifts of S_0 mode for these solutions are not apparent. These will make it possible to be only sensitive to the liquid viscosity except for the environmental temperature. This essay attempts to decouple the functions of A_{01}, A_{03} and S_0 modes to obtain the basic physical parameters (density and sound velocity, viscosity) with different liquid loading responses. From the values which have been reported from literature [32] we can also determine the types of the solution. This work provides a selective, sensitive method for the measurement of physical parameters to an unknown solution. It can be useful for label-free biosensors.

2. Working Principle

Multi-mode wave, such as A_{01} mode, S_0 mode and their harmonic ones (A_{03} mode, for example) can be excited in Lamb wave sensors and detected directly by using a pair of inter-digital transducers (IDTs) [33] located on the surface of the piezoelectric layer [34,35]. In liquid sensing, the liquid and IDT will be located on the two opposite sides of the membrane. For the A_{01} mode and the A_{03} mode, when the Lamb wave phase velocity is less than the liquid sound velocity, there are evanescent waves produced around the membrane-liquid interface. The phase velocity of the Lamb waves within the evanescent penetration field will be the same with the phase velocity inside the membrane. Taking account of the bending stiffness and the in-plane tension of the plate (B_i) for the A_{01} mode and the A_{03} mode, the phase velocity will be [31,36]:

$$c_{Pi} = \sqrt{B_i/(M + m_{Li})} \tag{1}$$

where i denotes 1 or 3 for the A_{0i} mode, B_i reflects the influences of the bending stiffness and the in-plane tension of the plate for the A_{0i} mode, M is the mass per unit area of the plate, the effective mass m_{Li} in the so-called evanescent penetration depth δ_{Ei} equals:

$$m_{Li} = \rho_L \delta_{Ei} \tag{2}$$

In which, ρ_L is the detected liquid density. The evanescent penetration depth δ_{Ei} obeys the following equation [37–39]:

$$\delta_{Ei} = \lambda_i \Big/ \left(2\pi\sqrt{1-(c_{Pi}/c_L)^2}\right) \tag{3}$$

where λ_i and c_{Pi} denote the Lamb wave wavelength and phase velocity respectively in each mode. c_L is the bulk acoustic velocity of the detected liquid. c_{Pi} is determined by the frequency (f_i) via $c_{Pi} = f_i \lambda_i$.

By substituting the Equations (2) and (3) into the Equation (1), we will get the following formula:

$$\rho_L \lambda_i \Big/ \left(2\pi\sqrt{1-(c_{Pi}/c_L)^2}\right) = B_i / c_{Pi}^2 - M \tag{4}$$

In this formula, the constants B_i, λ_i, and M are independent of the liquid type; λ_i is determined by the structure of the device. With the implicit Equation (4), the density and sound velocity of the liquid on the sensor can be decoupled when the frequency response of the A_{01} mode and the A_{03} mode are obtained by the experiments.

In the measurement, the relative frequency shifts ($\Delta f/f$) will be used frequently. By taking the term $c_{Pi} = f_i \lambda_i$ into Equation (1) and deriving of the equation, the value of $\Delta f/f$) for the A_{01} mode and the A_{03} mode will be:

$$\Delta f_i / f_i = -\Delta(\rho_L \delta_{Ei})/2M = -(\delta_{Ei}\Delta\rho_L + \rho_L \Delta\delta_{Ei})/2M \tag{5}$$

Obviously, the density and the sound velocity are the two factors affecting the relative frequency shifts. When the phase velocity is far less than the liquid sound velocity ($c_P \ll c_L$), such as the A_{01} mode, the values of δ_E and $\Delta\delta_E$ approach $\lambda/2\pi$ and 0, respectively. Then, in this situation the variations of the liquid sound velocity will have an almost negligible influence on the relative frequency shift. When the phase velocity is close to the liquid sound velocity, such as the A_{03} mode, the value $1 - (c_P/c_L)^2$ approaches 0. The influence of the terms δ_E and c_L cannot be neglected any more. The liquid density and sound velocity will simultaneously affect the frequency shifts. The value of $\Delta f/f$ can be positive or negative which depends on the sum of the value of $\rho_L \Delta\delta_E$ and the value of $\delta_E \Delta\rho_L$. Anyway, if we combine these two cases (A_{01} mode, A_{03} mode) simultaneously, we can get the values ρ_L and c_L with high sensitivity.

For the S_0 mode, when the wavelength of the Lamb mode is larger than the thickness of the plate, the phase velocity (c_p) for the principal symmetric mode can be simplified as [40]:

$$c_p = c_t \left[4\left(1 - \frac{c_t^2}{c_d^2}\right) \right]^{\frac{1}{2}} \left[1 + \frac{I}{2} \frac{\rho_L c_L^2}{\rho_m c_t^2} \frac{\omega d}{2c_L} \left(\frac{1}{4\left(1 - c_t^2/c_d^2\right)} - \frac{c_t^2}{c_d^2} \right) \right] \tag{6}$$

where c_d and c_t are the velocities of longitudinal (dilatational) and transverse (shear) waves of the membrane, c_L is the liquid sound velocity, ρ_m and ρ_L are the density of the solid membrane and liquid respectively, d is the membrane thickness, I denotes the square root of -1.

Evidently, the effect of liquid on the propagation of the S_0 mode does not change the real part of the phase velocity, but adds a very small attenuation of the amplitude [40]. This mode is suitable for the detection of attenuation. The amplitude (A_L) response of an unknown solution can be expressed by:

$$A_L = A_0 e^{-\alpha_{XL} x} \tag{7}$$

where the attenuation coefficient α_{XL} is proportional to $(\rho_L \eta_L)^{0.5}$, with η_L being the viscosity of the liquid. Similarly, the amplitude response (A_W) of water is given by:

$$A_W = A_0 e^{-\alpha_{XW} x} \tag{8}$$

In engineering, the insertion loss (dB) is widely used. The values of A_L and A_W can be transformed into values in dB scale which are denoted by A_{LdB} and A_{WdB}, respectively. Therefore, the attenuation difference (ΔA_{dB}) between an unknown solution and water can be expressed in dB scale as follows:

$$\Delta A_{dB} = A_{LdB} - A_{WdB} = \gamma_1 (\rho_L \eta_L)^{1/2} + \gamma_2 \tag{9}$$

in which both of the slope γ_1 and γ_2 are constant, and the constant γ_2 is determined by the reference liquid (water). As the density and the sound velocity of the solution can be estimated by both the frequency shifts of the A_{01} mode and the A_{03} mode, the multi-parameters (ρ_L, c_L, η_L) of the solution can be decoupled simultaneously with these three modes. According to these principles, a series of experiments were set up to investigate the responses of the multi modes of Lamb wave to the loading solutions.

3. Experiments for Liquid Detection

3.1. Experimental Setup

The micro Lamb wave device in Figure 1(a) contains a silicon membrane (length 7.8 mm, thickness ~12 μm) with a ground layer (Ti/Mo, GND, ~0.2 μm) and a piezoelectric layer (aluminum nitride, AlN, ~1.8 μm). Lamb waves are excited and detected directly using bidirectional inter-digital transducers (IDTs) [33] located on the surface of the AlN layer. There are six pairs of fingers on bidirectional IDTs in each exciting and detecting transducer. The period of bidirectional IDT is about 400 μm. As waves are partly reflected at the end of length-limited membrane (~7.8 mm), the device has strong signal without reflectors on both ends of the membrane. With the layers described as in [34], the mass per unit area of the membrane (M) is about 0.0355 kg/m^2.

The micro Lamb wave device is packaged directly with the printed circuit board (PCB), as shown in Figure 1(b). The network analyzer (Agilent 4395A), connected with the PCB, is used to excite and receive the acoustic signals. The device is protected with one cover on top of the system. The tube is used to pass the liquid into/out of the chamber, which is sealed up with the polymethyl methacrylate (PMMA) cover under the PCB.

Figure 1. The system for liquid detection, (**a**) Schematic diagram of the micro Lamb wave sensor interaction with liquid, ρ_L: density, c_L: sound velocity, η_L: viscosity; (**b**) Micro Lamb wave sensor packaged with printed circuit board (PCB).

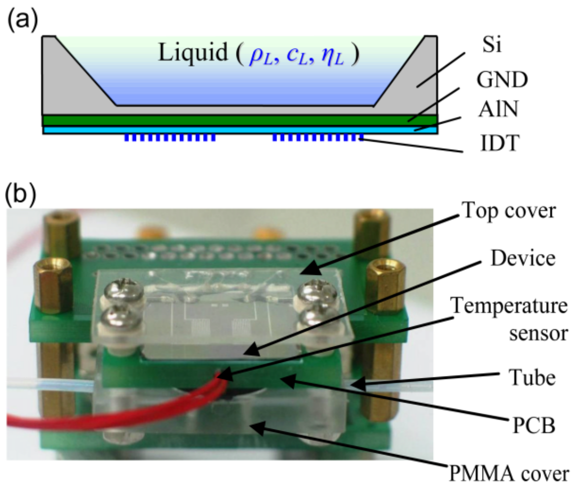

Figure 2. The responses of the A_{01} mode, the A_{03} mode, and the S_0 mode to the air and the water loading on the Lamb wave sensor.

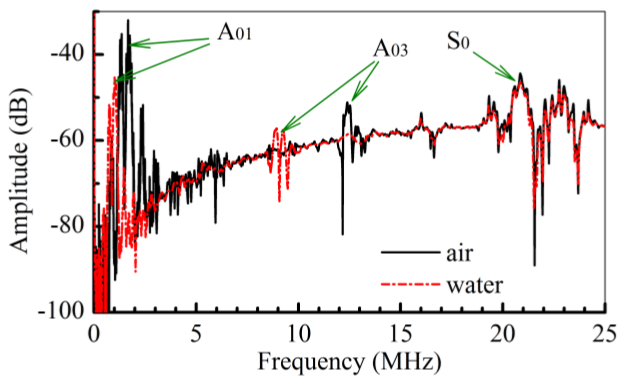

When the device is loaded with air or water, multi-modes can be excited and detected effectively, including the A_{01} mode, the A_{03} mode, and the S_0 mode (Figure 2). As the A_{01} and A_{03} modes are harmonic, the wavelength of the A_{03} mode is about one third of the wavelength of the A_{01} mode. According to the positions of the A_{01} mode, A_{03} mode and S_0 mode in the dispersion curves [41,42], the resonant frequencies (f) of these three modes should have the following relation: $f_{A01} < f_{A03} < f_{S0}$. The measured resonant frequency of the A_{01} and A_{03} modes for water loading are 0.987 and 9.233 MHz, respectively. With the frequency (f) and the wavelength (λ), the corresponding phase velocities ($f\lambda$) of these two modes are 385 m/s and 1,200 m/s respectively. Although the phase velocity of the A_{01} mode is far less than the sound velocity of water (1,485.5 m/s), it is close to the sound velocity of water for the A_{03} mode. With the same water loading for the S_0 mode, the measured central resonant frequency is about 20.86 MHz. The corresponding phase velocity of the S_0 mode is about 8,135.4 m/s. Further experiments were conducted to investigate the response of multi-modes to the different solutions.

3.2. Experiments for One Species Solutions (NaCl Solutions) with Different Concentrations

The first experiment was done to measure known solutions with different concentrations (Figure 3), such as NaCl solutions. When water is designated as the reference liquid, the relative frequency shifts ($\Delta f/f$ = ($f_{solution}$ − f_{water})/f_{water}) with concentration are different for these three modes (A_{01} mode, A_{03} mode, and S_0 mode), where $f_{solution}$ and f_{water} are the measured frequencies for the solution and the water, respectively. The frequency of the A_{01} mode decreases with the concentrations and the A_{03} mode behaves oppositely. In the case of the A_{03} mode of NaCl solutions measured in Figure 3, the absolute value $\rho\Delta\delta_E$ is bigger than the absolute value $\delta_E\Delta\rho$ (Table 1). This causes the positive frequency shifts of A_{03} mode in NaCl solutions measurements. In any case, when the frequency shift is positive, this means the Lamb wave phase velocity is close to the liquid sound velocity. In this case, this phenomenon can be used to decouple the liquid sound velocity.

Figure 3. Relative frequency shifts ($\Delta f/f$) for the A_{01} mode, the A_{03} mode, and the S_0 mode in the measurements of the NaCl solutions.

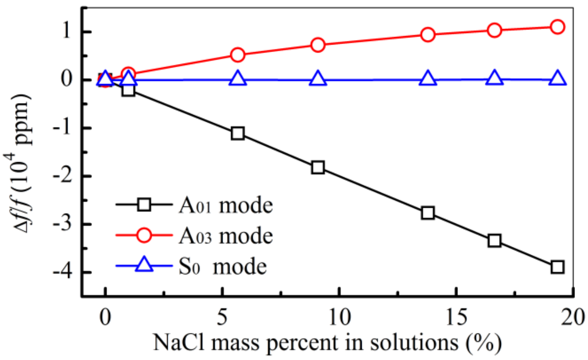

Table 1. Based on the measured frequency shifts of NaCl solutions measured in Figure 3, comparison of the value $\rho\Delta\delta_E$ and the value $\delta_E\Delta\rho$ for the A_{03} mode.

Concentration (%)	Density (10^3 kg/m^3)	c_P (m/s)	δ_E (μm)	$\delta_E\Delta\rho$	$\rho\Delta\delta_E$
0	0.9981	1,200.30	35.12	0	0
0.99	1.0052	1,201.71	34.70	0.25	−0.42
5.67	1.0389	1,206.55	32.81	1.34	−2.39
9.09	1.0640	1,209.03	31.58	2.08	−3.77
13.79	1.0995	1,211.59	30.01	3.04	−5.62
16.64	1.1212	1,212.69	29.13	3.59	−6.71
19.33	1.1425	1,213.53	28.40	4.10	−7.67

Compared with the frequency shifts measured with the A_{01} mode and A_{03} mode, the frequency of the S_0 mode shows negligible shift with different concentrations (Figure 3).

3.3. Experiments for Three Different Unknown Species Solutions

The second experiment was done to measure the modes' responses to three different species of aqueous electrolytic solutions with different concentrations (Table 2). We will check the possibility of the method to decouple the density and the acoustic sound velocity of these solutions with the measurements of A_{01} mode and A_{03} mode. Three different species of aqueous electrolytic solutions are prepared, they are listed as solution A, solution B, and solution C respectively, as it is shown in Table 2. From No. 1 to No. 6 solutions, they are the solution A. No. 7 and No. 8 solutions are the solution B. No. 9 and No. 10 are solution C. In each kind of solution, the concentration increases with the serial number. The S_0 mode is still insensitive to the solution changes compared with the measurement in water, and its values are not listed here.

Table 2. Relative frequency shifts (Δf/f) for the A_{01} mode and the A_{03} mode in the measurements of three kinds of unknown solutions. In each kind solution, the concentration increases with the serial number.

	Solution A						**Solution B**		**Solution C**	
No. of solutions	1	2	3	4	5	6	7	8	9	10
Concentration (%)	0.99	6.05	9.97	16.03	19.96	23.95	9.35	18.07	8.98	17.32
$\Delta f/f$ (A_{01} mode) (-1×10^4 ppm)	0.236	1.09	1.846	2.886	3.654	4.434	2.243	4.474	2.216	4.356
$\Delta f/f$ (A_{03} mode) (10^4 ppm)	0.027	0.216	0.357	0.373	0.325	0.287	−0.649	−1.422	−0.876	−1.848

In the case of solution A, the relative frequency shifts $\Delta f/f$ of A_{01} mode and A_{03} mode have similar properties with the solution of NaCl measured in Figure 3. But for the solution B and solution C, the relative frequency shifts of A_{03} mode is negative. As it is indicated in Equation (5), the absolute value $\rho\Delta\delta_E$ of solution B and solution C measured in Table 2 should be smaller than the absolute value $\delta_E\Delta\rho$.

Even for different kinds of solutions, such as the No. 6, No. 8, and No. 10 solutions, the values of $\Delta f/f$ of the A_{01} mode are almost the same, but the values of $\Delta f/f$ of the A_{03} mode are apparently different. This means only one antisymmetric mode measurement, such as A_{01} mode, can not determine the solution with high selectivity. In order to specify the liquid with high selectivity, it is better to decouple the liquid density and the liquid sound velocity with the measured relative frequency shifts of A_{01} mode and A_{03} mode. These will be analyzed in following section.

3.4. Viscosity Measurements with the S_0 Mode

The responses of the S_0 mode to the solutions of NaBr are similar to the ones of NaCl (Figure 3), the central frequency does not show apparent shifts due to their changing concentrations. However, the changes of the amplitude are related to the liquid's concentrations (Figure 4). It is because the frequency is mainly affected by the liquid density and sound velocity, which has no effects on the real part of the phase velocity of S_0 mode (Equation (6)) [40]. The amplitude of the S_0 mode in NaBr solution (Figure 4) shows that energy losses increase with the concentration, which is caused by the density and the viscosity of the liquid (Equation (7)). This can be used to decouple the density and the viscosity of the solution.

Figure 4. The responses of the S_0 mode to different concentrations of NaBr solutions.

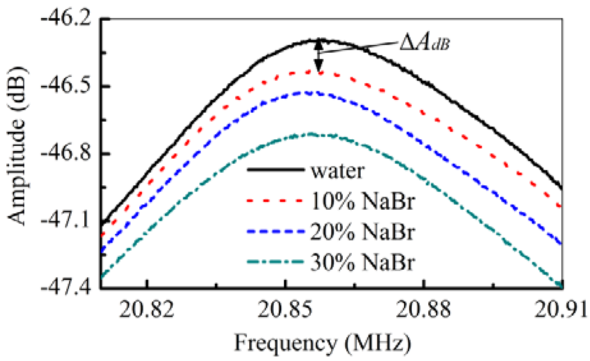

4. Results and Discussions

4.1. To Decouple the Density and the Acoustic Sound Velocity with the A_{01} Mode and A_{03} Mode

In order to specify the liquid with high selectivity, we attempted to decouple the liquid density and the liquid sound velocity with the measured frequency shifts of A_{01} mode and A_{03} mode. Based on the Equation (4), two steps are undertaken in order to decouple the density and the sound velocity of a liquid as follows:

(1) Determine the constant B_i by measuring the frequency response of the reference liquid. Here, the water works as the reference liquid, the values of B_1 and B_3 are 14,767.3 N/m and 101,642.8 N/m respectively.
(2) Get the physical parameters (ρ_L, c_L) for a unknown liquid by measuring c_{Pi}. All other parameters (B_i, λ_i, M) in Equation (1) have already been calculated or measured.

The first decoupled result using Equation (1) is the NaCl solution with different concentrations, as measured in Figure 3. Comparing the measured density and sound velocity with the values from the literature [32], the two results are close, as shown in Figure 5.

Figure 5. The decoupled density and sound velocity of NaCl solutions and other solutions using measurements in A_{01} mode and A_{03} mode.

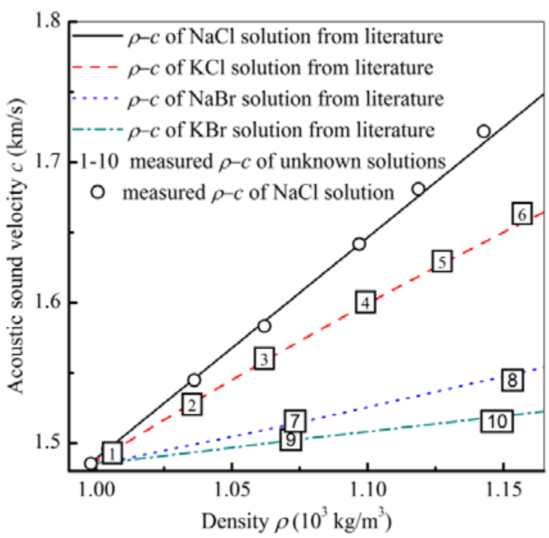

Based on the same process, the density and the sound velocity for other three different species solutions with different concentrations were also decoupled and are shown in Figure 5. Compared with the values from the literature [32], No. 1–No. 6 solutions are KCl solutions, No. 7 and No. 8 solutions are NaBr solutions, and No. 9 and No. 10 solutions are KBr solutions. Aside from decoupled density and sound velocity, the species of the solutions can be identified by comparing the measured values with the already known values [32]. After these density and sound velocity being decoupled using A_{01} mode and A_{03} mode, the liquid are determined with higher selectivity compared with only A_{01} mode measurement.

For Nos. 6, 8, and 10 solutions, the decoupled densities (Figure 5) are almost the same because the relative frequency shifts are very close (Table 2). For these solutions with adjacent density, sound velocities become the main factors affecting the frequency shifts in the A_{03} mode (Table 2). With the relations of the absolute frequency shifts: $\Delta f/f_{No.6} > \Delta f/f_{No.8} > \Delta f/f_{No.10}$ (Table 2), the decoupled sound velocity of these three solutions have the following relation: $c_{No.6} > c_{No.8} > c_{No.10}$ (Figure 5).

4.2. The Linear Response of (Density × Viscosity)$^{0.5}$ Changing with the Item of Amplitude Shifts (ΔA_{dB}) in S_0 Mode

The item (density × viscosity)$^{0.5}$ changes almost linearly with the item of amplitude shifts (ΔA_{dB}), and the linear fitting coefficient is about 1.02 ± 0.09 (dB/(kg·m^{-2}·s$^{-0.5}$)), such as the NaBr and NaCl solutions (Figure 6). Beside the density and the viscosity, other parameters, such as the liquid's conductivity, affect the amplitude shifts. This is maybe the reason why the high linearity of (density × viscosity)$^{0.5}$ doesn't change with the amplitude shift. However, by analyzing the amplitude shifts (ΔA_{dB}) of the S_0 mode, the viscosity of the solution can be derived. With the determined density by measuring the frequency response of the A_{01} and A_{03} modes, the viscosity will be determined by checking the amplitude response in the S_0 mode.

Figure 6. Amplitude shifts *versus* (density × viscosity)$^{0.5}$ for the NaCl and NaBr solutions in the S_0 mode.

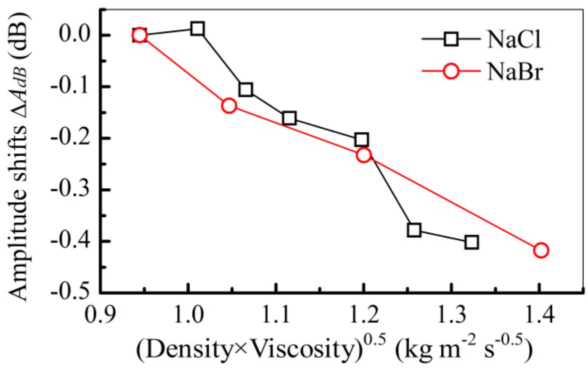

5. Conclusions

In this study, for the first time to our knowledge, the density, sound velocity, and viscosity of the liquid are obtained simultaneously based on the measurements of the same solution sample volume with a Lamb wave sensor. When the frequency shifts of the A_{01} and A_{03} modes are combined, the density and sound velocity are decoupled. This happens because the phase velocity of the A_{01} mode is far from the sound velocity of the liquid and the phase velocity of the A_{03} mode is close to the sound velocity of the liquid. Viscosity is obtained by measuring the amplitude of the S_0 mode, which is especially suitable for Newtonian fluids. Effects of the aqueous electrolytic solutions' conductivity on these three modes are not clearly observed. The term (density × viscosity)$^{0.5}$ doesn't show high linearity as a function of amplitude shifts.

However, with this multi-parameter detection method, unknown solutions such as aqueous electrolytic solutions can be distinguished successfully and with high selectivity. Results clearly indicate that the multi-modes of a micro Lamb wave sensor are promising in the investigation of molecular thermodynamics, adiabatic compressibility, and molecular label free detection, among others.

Acknowledgement

The authors gratefully acknowledge the technical support from Engineers Jean-Yves Rauch of Femto-st, Pascal Blind of CTMN (Besançon), and Feng Li of CIOMP. Parts of the present work were financially supported by the National Natural Science Foundation of China (Nos. 11034007, 60971025) and the Chinese Academy of Sciences Innovation Program (KJCX2-YW-H18).

References

1. Fu, Y.Q.; Luo, J.K.; Du, X.Y.; Flewitt, A.J.; Li, Y.; Markx, G.H.; Walton, A.J.; Milne, W.I. Recent developments on ZnO films for acoustic wave based bio-sensing and microfluidic applications: A review. *Sens. Actuators B* **2010**, *143*, 606–619.
2. Hager, H.E. Fluid property evaluation by piezoelectric crystals operating in the thickness shear mode. *Chem. Eng. Commun.* **1986**, *43*, 25–38.
3. Kondoh, J.; Shiokawa, S. Measurements of conductivity and pH of liquid using surface acoustic wave devices. *Jpn. J. Appl. Phys.* **1992**, *31*, 82–84.
4. Lau, O.-W.; Shao, B.; Zhang, W. Evaluation of methods to minimize effects of liquid viscosity and density on the oscillating frequencies of thickness-shear-mode (TSM) piezoelectric resonators. *Anal. Chim. Acta* **1995**, *312*, 217–222.
5. Arapan, L.; Alexieva, G.; Avramov, I.D.; Radeva, E.; Strashilov, V.; Katardjiev, I.; Yantchev, V. Highly mass-sensitive thin Film Plate Acoustic Resonators (FPAR). *Sensors* **2011**, *11*, 6942–6953.
6. Sarvazyan, A.P. Ultrasonic velocimetry of biological compounds. *Annu. Rev. Biophys. Biophys. Chem.* **1991**, *20*, 321–342.
7. Martin, S.J.; Ricco, A.J.; Niemczyk, T.M.; Frye, G.C. Characterization of SH acoustic plate mode liquid sensors. *Sens. Actuators* **1989**, *20*, 253–268.
8. Montagut, Y.; García, J.V.; Jiménez, Y.; March, C.; Montoya, Á.; Arnau, A. Validation of a phase-mass characterization concept and interface for acoustic biosensors. *Sensors* **2011**, *11*, 4702–4720.
9. Kovacs, G.; Vellekoop, M.J.; Haueis, R.; Lubking, G.W.; Venema, A. A love wave sensor for (bio)chemical sensing in liquids. *Sens. Actuators A* **1994**, *43*, 38–43.
10. Newton, M.; Roach, P.; McHale, G. ST quartz acoustic wave sensors with sectional guiding layers. *Sensors* **2008**, *8*, 4384–4391.

11. Länge, K.; Rapp, B.; Rapp, M. Surface acoustic wave biosensors: A review. *Anal. Bioanal. Chem.* **2008**, *391*, 1509–1519.
12. Rocha-Gaso, M.-I.; March-Iborra, C.; Montoya-Baides, A.; Arnau-Vives, A. Surface generated acoustic wave biosensors for the detection of pathogens: A review. *Sensors* **2009**, *9*, 5740–5769.
13. Voiculescu, I.; Nordin, A.N. Acoustic wave based MEMS devices for biosensing applications. *Biosens. Bioelectron.* **2012**, *33*, 1–9.
14. Priego Capote, F.; Luque de Castro, M. Ultrasound in analytical chemistry. *Anal. Bioanal. Chem.* **2007**, *387*, 249–257.
15. Cooper, M. Label-free screening of bio-molecular interactions. *Anal. Bioanal. Chem.* **2003**, *377*, 834–842.
16. Rocha-Gaso, M.-I.; March-Iborra, C.; Montoya-Baides, Á.; Arnau-Vives, A. Surface generated acoustic wave biosensors for the detection of pathogens: A review. *Sensors* **2009**, *9*, 5740–5769.
17. Rapp, B.; Gruhl, F.; Länge, K. Biosensors with label-free detection designed for diagnostic applications. *Anal. Bioanal. Chem.* **2010**, *398*, 2403–2412.
18. Hino, R.; Esashi, M.; Tanaka, S. Antisymmetric-mode Lamb wave methanol sensor with edge reflectors for fuel cell applications. In *Proceedings of the 23rd IEEE International Conference on Micro Electro Mechanical Systems, Technical Digest (MEMS 2010)*, Hong Kong, 24−28 January 2010; pp. 871–874.
19. Latif, U.; Mujahid, A.; Afzal, A.; Sikorski, R.; Lieberzeit, P.; Dickert, F. Dual and tetraelectrode QCMs using imprinted polymers as receptors for ions and neutral analytes. *Anal. Bioanal. Chem.* **2011**, *400*, 2507–2515.
20. Raimbault, V.; Rebiere, D.; Dejous, C.; Guirardel, M.; Lachaud, J.L. Molecular weight influence study of aqueous poly(ethylene glycol) solutions with a microfluidic Love wave sensor. *Sens. Actuators B* **2010**, *144*, 318–322.
21. Herrmann, F.; Hahn, D.; Büttgenbach, S. Separate determination of liquid density and viscosity with sagittally corrugated Love-mode sensors. *Sens. Actuators A* **1999**, *78*, 99–107.
22. Doy, N.; McHale, G.; Newton, M.I.; Hardacre, C.; Ge, R.; MacInnes, J.M.; Kuvshinov, D.; Allen, R.W. Small volume laboratory on a chip measurements incorporating the quartz crystal microbalance to measure the viscosity-density product of room temperature ionic liquids. *Biomicrofluidics* **2010**, doi:10.1063/1.3353379.
23. Mitsakakis, K.; Tsortos, A.; Kondoh, J.; Gizeli, E. Parametric study of SH-SAW device response to various types of surface perturbations. *Sens. Actuators B* **2009**, *138*, 408–416.
24. Oita, I.; Halewyck, H.; Thys, B.; Rombaut, B.; Vander Heyden, Y.; Mangelings, D. Microfluidics in macro-biomolecules analysis: Macro inside in a nano world. *Anal. Bioanal. Chem.* **2010**, *398*, 239–264.
25. Laurent, T.; Bastien, F.O.; Pommier, J.-C.; Cachard, A.; Remiens, D.; Cattan, E. Lamb wave and plate mode in ZnO/silicon and AlN/silicon membrane: Application to sensors able to operate in contact with liquid. *Sens. Actuators A* **2000**, *87*, 26–37.
26. Jia, H.; Duhamel, R.; Manceau, J.F.; de Labachelerie, M.; Bastien, F. Improvement of Lamb waves sensors: Temperature sensitivity compensation. *Sens. Actuators A* **2005**, *121*, 321–326.

27. Choujaa, A.; Tirole, N.; Bonjour, C.; Martin, G.; Hauden, D.; Blind, P.; Cachard, A.; Pommier, C. AlN/silicon Lamb-wave microsensors for pressure and gravimetric measurements. *Sens. Actuators A* **1995**, *46*, 179–182.
28. Moll, J.; Golub, M.V.; Glushkov, E.; Glushkova, N.; Fritzen, C.-P. Non-axisymmetric Lamb wave excitation by piezoelectric wafer active sensors. *Sens. Actuators A* **2012**, *174*, 173–180.
29. Rizwaan, A. Time-space analysis of a surface-bonded piezoelectric film's response with Lamb wave for diagnostics. *Sens. Actuators A* **2010**, *161*, 12–22.
30. Li, F.; Wu, Y.; Manceau, J.-F.; Bastien, F. Temperature compensation of Lamb wave sensor by combined antisymmetric mode and symmetric mode. *Appl. Phys. Lett.* **2008**, *92*, 074101:1–074101:3.
31. Martin, B.A.; Wenzel, S.W.; White, R.M. Viscosity and density sensing with ultrasonic plate waves. *Sens. Actuators A* **1990**, *22*, 704–708.
32. Freyer, E.B. Sonic studies of the physical properties of liquids. II. The velocity of sound in solutions of certain alkali halides and their compressibilities. *J. Am. Chem. Soc.* **1931**, *53*, 1313–1320.
33. White, R.M.; Voltmer, F.W. Direct piezoelectric coupling to surface elastic waves. *Appl. Phys. Lett.* **1965**, *7*, 314–316.
34. Zhou, L.; Manceau, J.-F.; Bastien, F. Influence of gases on Lamb waves propagations in resonator. *Appl. Phys. Lett.* **2009**, *95*, 223505–223507.
35. Zhou, L.; Manceau, J.-F.; Bastien, F. Interaction between gas flow and a Lamb waves based microsensor. *Sens. Actuators A* **2012**, *181*, 1–5.
36. Chen, Z.; Han, T.; Shi, W.; Ji, X.; Li, L. Separate determination of liquid properties with Lamb wave devices. In *Proceedings of the 2006 IEEE International Frequency Control Symposium and Exposition*, Miami, FL, USA, 4–7 June 2006; Volumes 1–2, pp. 322–327.
37. Moroney, R.M.; White, R.M.; Howe, R.T. Microtransport induced by ultrasonic Lamb waves. *Appl. Phys. Lett.* **1991**, *59*, 774–776.
38. Nguyen, N.T.; White, R.M. Design and optimization of an ultrasonic flexural plate wave micropump using numerical simulation. *Sens. Actuators A* **1999**, *77*, 229–236.
39. Sayar, E.; Farouk, B. Acoustically generated flows in microchannel flexural plate wave sensors: Effects of compressibility. *Sens. Actuators A* **2011**, *171*, 317–323.
40. Osborne, M.F.M.; Hart, S.D. Transmission, reflection, and guiding of an exponential pulse by a steel plate in water. I. theory. *J. Acoust. Soc. Am.* **1945**, *17*, 1–18.
41. Leckey, C.A.C.; Rogge, M.D.; Miller, C.A.; Hinders, M.K. Multiple-mode Lamb wave scattering simulations using 3D elastodynamic finite integration technique. *Ultrasonics* **2012**, *52*, 193–207.
42. Zhu, Z.; Wu, J.; Li, J.; Zhou, W. A general dispersion relation for Lamb-wave sensors with liquid-layer loading. *Sens. Actuators A* **1995**, *49*, 79–84.

© 2012 by the authors; licensee MDPI, Basel, Switzerland. This article is an open access article distributed under the terms and conditions of the Creative Commons Attribution license (http://creativecommons.org/licenses/by/3.0/).